degradation rate of Rs accelerates to a $t_{1/2}$ of 3 days (see the figure) but restabilizes after reinnervation. Accelerated degradation of Rs is also seen in dystrophin-deficient *mdx* mice, which are a model for muscular dystrophy in humans (*8*). Thus instability of Rs may be a general feature of various pathologic conditions.

AChRs are internalized and degraded via the lysosomal pathway (*9*) but the membrane route that AChRs take has been a matter of speculation. The perijunctional region of the NMJ has long been known to have a higher receptor density than the rest of the muscle membrane (*10*). An early model suggested that receptors at the NMJ cannot be degraded while anchored in the muscle membrane and that the degradation rate depends on the affinity of the receptors for these anchoring sites. Once detached from their anchors, the receptors are free to diffuse in the membrane and can move to the perijunctional region where they are internalized (*7*). This model allows for receptors with different degradation rates to reside side by side in the membrane, which is in fact the case at the NMJ. Akaaboune *et al.* lend support to this hypothesis by showing that the perijunctional region serves as a way-station in normal AChR turnover receiving both new receptors and those destined for degradation.

After AChRs are saturated with the snake venom α-bungarotoxin, there is an initial, rapid ($t_{1/2} < 1$ day) increase in degradation rate. While one hypothesis to explain this phenomenon—that Rs are degraded rapidly when first inserted into the postsynaptic muscle membrane but then are stabilized by nerve activity—has been disproved (*11*), no alternate satisfactory mechanism has been proposed. Now Akaaboune *et al.* solve this long-standing puzzle by showing that it is the full inactivation of AChRs that is the cause of accelerated Rs degradation. Electrical stimulation of the muscle prevents this and also prevents the acceleration of Rs degradation after denervation (*12*). Thus, the nerve can regulate AChR stability by activating muscle contraction.

What are the functional consequences of maintaining a high density of stable receptors at the NMJ? A high AChR concentration close to the nerve terminal enables acetylcholine to act over a small distance at saturating concentrations, providing efficient binding of neurotransmitter to AChRs and the initiation of muscle contraction. The location of the enzyme acetylcholine esterase close to the receptors enables quick termination of acetylcholine activity, thus allowing the muscle to be activated repeatedly (*13*).

Much regarding the regulation of AChR turnover still remains to be clarified. Why is receptor degradation after prolonged denervation (when Schwann cells no longer release acetylcholine) slower ($t_{1/2} \sim 3$ to 4 days) than that induced by complete inactivation of AChRs ($t_{1/2} << 1$ day) by α-bungarotoxin? How does direct stimulation of muscle maintain receptor stability and how is calcium involved? How do the mechanisms involved in maintaining a high receptor density at the NMJ adapt to transitions, such as those in development or during reinnervation? If during such periods, rapidly degrading receptors are removed before they are fully replaced by receptors with a slower turnover, the decrease in receptor number could reduce the ability of the muscle to respond to nerve stimulation. Finally, fast synapses in the brain, where similarities with the NMJ are already emerging (*14*), also necessitate high receptor densities in the postsynaptic neuronal membrane. The similarities and differences in regulation of these two synaptic organizations will be the focus of studies for many years to come.

References and Notes

1. M. Akaaboune, J. W. Lichtman, S. Culican, S. Turney, *Science* **286**, 503 (1999).
2. J. R. Sanes and J. W. Lichtman, *Annu. Rev. Neurosci.* **22**, 389 (1999); Z. W. Hall and J. R. Sanes, *Cell 72/Neuron* **10** (suppl.), 99 (1993).
3. S. L. Shyng and M. M. Salpeter, *J. Neurosci.* **10**, 3905 (1990).
4. U. J. McMahan, *Cold Spring Harbor Symp. Quant. Biol.* **55**, 407 (1990); G. D. Fischbach and K. M. Rosen, *Annu. Rev. Neurosci.* **20**, 429 (1997).
5. Z. Z. Wang *et al.*, *J. Neurosci.* **19**, 1998 (1999); S. C. Froehner *et al.*, *Neuron* **5**, 403 (1990).
6. M. T. Meier *et al. J. Cell Biol.* **141**, 715 (1998).
7. M. M. Salpeter and R. H. Loring, *Prog. Neurobiol.* **25**, 297 (1985).
8. R. Xu and M. M. Salpeter, *J. Neurosci.* **17**, 8194 (1997).
9. D. Fambrough, *Physiol. Rev.* **599**, 165 (1979); G. Fumagalli *et al.*, *J. Neurophathol. Expl. Neurol.* **41**, 567 (1982); R. Xu and M. M. Salpeter, *J. Cell Physiol.* **181**, 107 (1999).
10. M. M. Salpeter *et al.*, *J. Cell Biol.* **106**, 2087 (1988).
11. D. A. Ramsay *et al.*, *Brain Res.* **581**, 198 (1992); J.R. Stiles and M. M. Salpeter, *Neuroscience* **78**, 895 (1997).
12. J. S. Andreose *et al.*, *J. Neurosci.* **13**, 3433 (1993).
13. M. M. Salpeter, *The Vertebrate Neuromuscular Junction*, M. M. Salpeter, Ed. (Liss, New York, 1987), pp. 35–43.
14. A. L. Mammen *et al.*, *J. Neurosci.* **17**, 7351 (1997).

I would like to thank W. Randall, E. Salpeter, and T. Podleski. Supported by NIH grant NS09315.

PERSPECTIVES: ASTROPHYSICS

The Complexity of Stellar Death

Yervant Terzian

Before the Hubble Space Telescope (HST), with its superior angular resolution, sensitivity, and dynamic range, began sending back images of stars in various stages of their life cycles, the death of a small star—such as our sun—was believed to be accompanied by formation of a smoothly expanding nebula. Now, dozens of spectacular images of planetary and protoplanetary nebulae provided by HST (*1*) have revealed morphological aspects completely unsuspected before (*2*). The newly found complexity represents a challenge for researchers trying to understand the mechanisms of stellar death.

The author is at the David C. Duncan Professor in the Physical Sciences in the Department of Astronomy at Cornell University, Space Sciences Building, Ithaca, NY 14853, USA. E-mail: terzian@astrosun.tn.cornell.edu

When a sunlike star, with a mass of up to a few solar masses, reaches the last stages of its evolution, it expands and becomes a cool (about 2500 K) red giant, with a size so large that its outer perimeter could include the orbit of Mars. This asymptotic giant branch (AGB) star loses mass in the form of stellar wind, followed by a more intense mass loss as a result of what is known as a superwind. The star hereby loses a substantial fraction of its mass, and the ejected material forms a planetary nebula. The stellar core contracts and becomes a white dwarf star (about the size of Earth, with a density of $\sim 10^7$ g/cm^3) with surface temperatures reaching about 10^5 K.

The material ejected from the star mostly initially consists of atomic and molecular gas, which partly coalesces shortly after ejection to form warm dust particles. Molecular species such as H_2, OH, CO, and SiO have been detected around many proto–planetary nebulae and in the envelopes of AGB stars (*3*). Dust surrounding the star absorbs starlight, and after reprocessing it emits strongly in the infrared.

Eventually, the hot white dwarf's ultraviolet radiation ionizes the nebula, which begins to emit strongly in the recombination lines of hydrogen and helium and spectral lines characteristic for doubly ionized oxygen, singly ionized nitrogen, and other ionized species. Within a few tens of thousands of years, the expanding planetary nebula diffuses into the interstellar medium with a velocity of ~ 20 km/s.

These stellar outbursts play an important role in the chemical evolution of our galaxy. It is estimated that they contribute at least 20 solar masses per century of stellar material to the interstellar medium; a comparable amount is provided by the more violent supernova explosions. The material ejected from both dying stars and supernovae contains heavier elements produced from hydrogen and helium by nucleosynthesis in the core of the stars.

The general stages of the late stellar evolution are reasonably well understood, but the mechanisms by which these old stars eject their envelopes remain mysterious, and we have been unable to understand what factors contribute to creating a particular nebular morphology. Not one of the images provided by the HST observations, performed with the Wide Field Planetary Camera 2, shows a simple expanding bubble. Most objects have complex bipolar structures with central torii, multipolar bubbles, jetlike filaments, and globules. Several objects even show sets of circular rings. Many nebulae show a detailed point and mirror symmetry that spans as far as 100,000 astronomical units from the central star (see the figures). Microstructures in planetary nebulae include ansae (outer extensions) and FLIERS (fast low-ionization emission regions) (*4*). The latter are low-ionization knots of small size (on the order of 10^{15} cm). They are easily seen in the nitrogen emission lines and tend to come in pairs that are equidistant from the central star and on opposite sides, normally in the directions of the nebular major axis. Kinematic studies of FLIERS (*5*) have shown that these structures are moving away from the central star with a velocity typically a few times that of the expansion of the nebula.

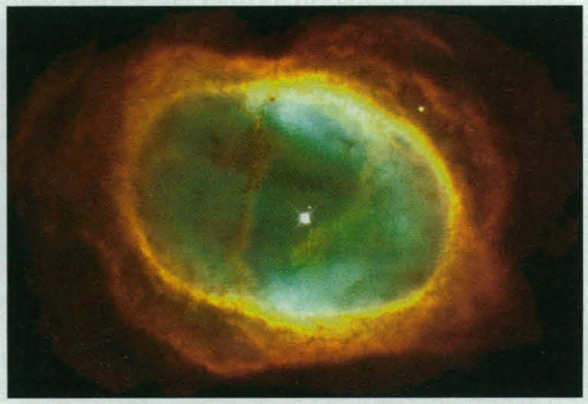

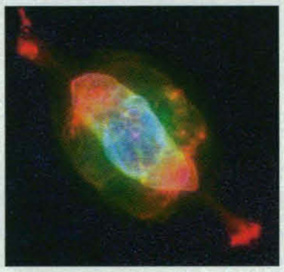

Unsuspected diversity. Images from the HST show detailed morphologies of planetary nebulae: bipolar structures (**above**), an elliptical structure with a binary central star (**top right**), and FLIERS (**bottom right**).

The HST images of planetary nebulae also show multiple faint concentric rings around some central stars. These rings appear to be concentric spherical shells that may have resulted from episodic mass loss from the AGB star, with periods of a few hundred to a thousand years. As many as 15 rings exist in the nebula CRL 2688, and 11 rings are seen in NGC 6543. CRL 2688 is primarily a reflection nebula in which the central star is surrounded by dust and starlight escapes along two opposite directions, forming a pair of bright nebulosities (see figure at right). These beams are interrupted by numerous concentric arcs, some of which can be traced all around the central object (*6*). In contrast, the rings around NGC 6543 seem to consist of ionized hot gas (*7*), indicating that the outer rings are ~10,000 years old but have not diffused out by thermal pressure. The ejection of the shells from the central star may not be directly associated with the stellar thermal pulses that result from succesive mucleosynthesis in the core of the star known as the "helium flash," because these are predicted to occur at much longer time intervals compared to the ejections of the rings. However, these theoretical predictions should be carefully reexamined.

Concentric arcs. Images of the CRL 2688 nebula show concentric rings and bipolar structure.

The HST has also been able to detect the small (~2 milli–arc seconds per year) angular expansion of planetary nebulae (*10*). Comparison of two images of the same object taken a few years apart has revealed measurable angular expansions. In conjunction with the Doppler expansion velocities, geometric distances to these objects have been obtained.

Researchers have considered the effects of stellar rotations, photoionization heating, and magnetic fields as possible mechanisms that result in the observed nebular morphologies (*8*). Hydrodynamical and magnetohydrodynamical simulations of single stars at the end of their AGB phases show a multitude of morphologies, from bipolar shapes to collimated butterfly structures. If sufficiently strong magnetic fields are used, ansae and jetlike features also clearly appear. Although these model results are very interesting, they require a magnetic field and a substantial stellar rotation at the tip of the AGB phase. The origin of significant stellar rotation and the required magnetic field strengths are not well understood.

Another promising approach in producing bipolar planetary nebulae considers the gravitational effects of a secondary star in close binary stellar systems where one evolved star begins to shed mass (*9*). The gravitational field of the companion star can indeed distribute the ejected material from the central star of the planetary nebula into a disk-shaped configuration, and when seen edge-on, the nebula appears to have a bipolar structure.

The HST observations have greatly enriched our knowledge about the death of sunlike stars. The new discoveries illustrate the complexity of stellar explosions near their deaths and pose a multitude of new questions for observers and theorists alike.

References and Notes

1. See Web site by A. Hajian and Y. Terzian at http://aries.usno.navy.mil/ad/pne/
2. Y. Terzian and A. Hajian, *Asymmetrical Planetary Nebulae* (Astronomical Society of the Pacific, in press).
3. P. J. Huggins, in *Planetary Nebulae*, R. Weinberger and A. Acker, Eds. (Kluwer, Dordrecht, 1993), pp. 147–154; S. Deguchi, in *Planetary Nebulae*, H. J. Habing and H. Lamers, Eds. (Kluwer, Dordrecht, 1997), pp. 151–160.
4. A. Hajian, B. Balick, Y. Terzian, M. Perinotto, *Astrophys. J.* **487**, 304 (1997); B. Balick *et al.*, *Astron. J.* **116**, 360 (1998).
5. B. Balick, H. L. Preston, V. Icke, *Astron. J.* **94**, 1641 (1987).
6. R. Sahai *et al.*, *Astrophys. J.* **493**, 301 (1998).
7. B. Balick and J. Wilson, in preparation.
8. G. Garcia-Segura, N. Langer, M. Rozyczka, J. Franco, *Astrophys. J.* **517**, 767 (1999).
9. M. Livio, J. Salzman, G. Shaviv, *Mon. Not. R. Astron. Soc.* **188**, 1 (1979); M. Morris, *Astrophys. J.* **249**, 572 (1981); N. Soker and A. Harpaz, *Publ. Astron. Soc. Pac.* **104**, 923 (1992); N. Mastrodemos, thesis, University of California, Los Angeles (1998).
10. D. S. Reed *et al.*, *Astron. J.*, in press.

CREDIT: AS IN (7), TELESCOPE SCIENCE INSTITUTE, NASA